Australasian Physical & Engineering Sciences in Medicine (2019) 42:553–561
https://doi.org/10.1007/s13246-019-00756-3

SCIENTIFIC PAPER

Quantitative analysis of effects of the grid specifications on the quality of digital radiography images

Sanghyun Lee[1] · **Woohyun Chung**[1]

Received: 19 August 2018 / Accepted: 2 April 2019 / Published online: 15 April 2019

Abstract

A grid is one of the key components of a digital radiography (DR) system because it removes scattered radiation, which arises when X-rays penetrate an object and improves diagnostic accuracy by enhancing image quality. With the widespread use of DR systems, demand for grids with high precision has simultaneously increased. Because unsuitable grids may decrease image quality and lead to misdiagnosis, using optimised grids for DR systems is critical. In this study, we aimed to analyse the quality of X-ray images acquired using grids with different specifications and proposed standardised criteria for grid use on the basis of our results. We measured modulation transfer function (MTF), normalised noise power spectrum (NNPS) and detective quantum efficiency (DQE) using grids with different ratios (10:1, 12:1 and 15:1) with or without implementing poly methyl methacrylate (PMMA) phantoms (0–20 cm). Pixel pitch of the detector used in this experiment was 143 µm. Based on this, a grid with a line frequency of 85 line pairs/cm was selected to prevent distortion caused by implementing unoptimised grids. As a result, the NNPS was found to increase when using the grid, and the difference in MTF and DQE was only measured when the scattered X-ray was generated by stacking the PMMA phantom. However, grids showed a positive effect MTF and DQE when the PMMA phantom was implemented. Specifically, MTF and DQE improved with increase in grid ratio. Thus, it is desirable to use a high-ratio grid to improve image quality.

Keywords Digital radiography · Grid · Grid ratio · Modulation transfer function · Detective quantum efficiency · Normalised noise power spectrum

Introduction

Since 1913, grids have been used to remove scattered radiation and to improve images quality in radiography [1]. Scattering radiation means refracted X-rays that lose their original linearity due to the interaction of the object with X-rays when X-rays pass through an object (Compton scattering). If this scattered radiation is detected by the detector, it makes the images unclear, thereby degrading image quality. Figure 1 presents the overall system for acquiring X-ray images using a grid in a digital radiography (DR) system. A grid is placed between the detector and subject, and it contributes to increasing the diagnostic accuracy by removing scattered radiation [2–4].

✉ Sanghyun Lee
leesh@jpi.co.kr

[1] R&D, JPI Healthcare, Co., Ltd., 43, Seonggok-ro 22beon-gil, Ansan-si, Republic of Korea

Figure 2 shows grid structure. A grid comprises absorbers and interspacers. An absorber is made of high-density materials such as lead or tungsten to remove the scattered radiation. In contrast, an interspacer is made of low-density materials, such as carbon fiber or aluminum, to transmit primary radiation. Line frequency refers to the number of pairs of absorbers and interspacers per unit distance, with a unit of either line pairs/cm (LP/cm) or line pairs/inch (LP/in). Line frequency is the most critical factor determining the occurrence of the moiré pattern, which arises when an unoptimised grid is implemented in a DR system. Each detector comprises a pixel matrix that can detect X-rays. The size of pixels in a detector determines the spatial resolution of the detector. The spatial resolution of a detector and line frequency of a grid can be represented by the concept of spatial frequency. When the spatial frequencies of a detector and grid do not match, a new signal with a unique frequency is created. This signal results in a distorted pattern called the moiré pattern [5–8].

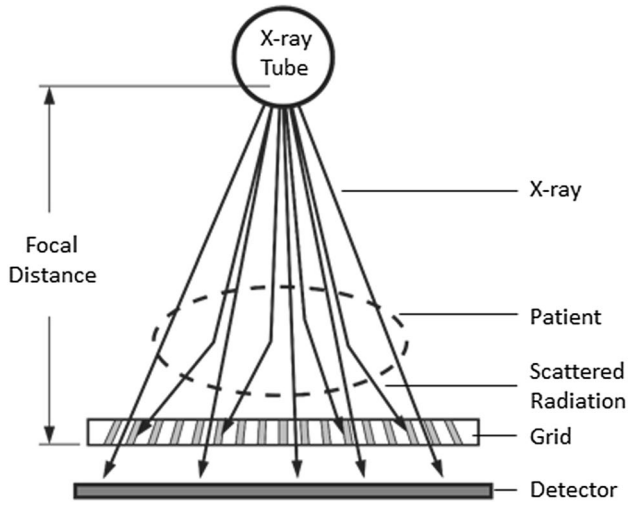

Fig. 1 Acquisition of an X-ray image using a grid in a digital radiography system

To remove the moiré pattern, an optimised grid should be used. The process for determining the optimised grid is as follows: a) select two or three grids with different line densities based on specifications of the DR system, such as focal spot size, pixel size, or scintillator in the detector; b) acquire images using the selected grids; c) perform visual inspection of the acquired images and analyse the images in the frequency domain; and d) determine the grid with the line frequency that best fits the DR system. Thus, determination of an optimised grid is heavily dependent on the specifications of the DR system.

In a grid, each line pair of interspacers and absorbers is aligned at a certain angle in the direction of the X-ray source, maintaining the linearity of the X-ray. This angle is determined by focal distance (FD), which is the distance between X-ray tube focus and bottom surface of the grid. In general, FD is identical to the source-to-image receptor distance (SID) of the DR system. FD and SID are dependent on the body part of image acquisition.

Grid ratio is the ratio of the height of the grid (H) to the width of an interspacer (D). The higher the grid ratio, the less scattered radiation reaching the detector; conversely, the lower the grid ratio, the more primary X-rays transmitted through the grid. Thus, the use of grid with an incorrect ratio for a DR system leads to redundant doses or reduced contrast. Unlike line frequency and FD, grid ratio can be determined independent of clinical diagnosis environment and DR system configuration. However, precise grid ratio

Fig. 2 Grid structure

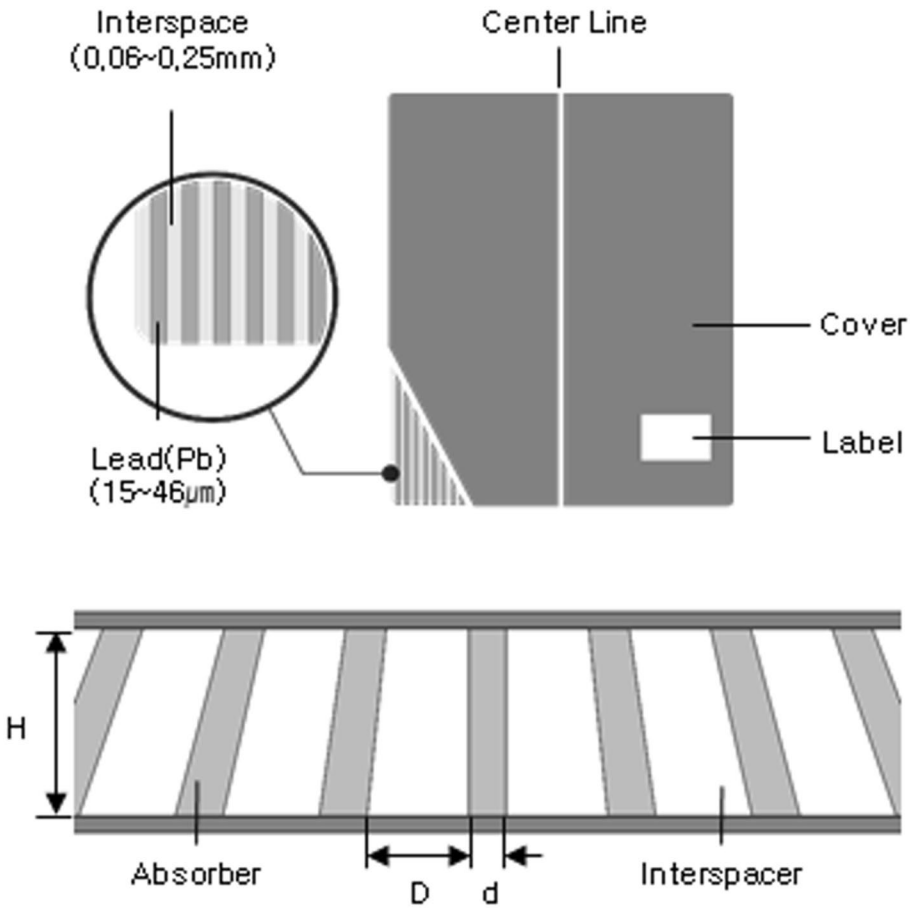

should be determined as it is directly related to image quality and exposure dose in a patient [9, 10]. Previous research has mainly focused on measuring physical grid characteristics along the grid type or simulations using the Monte Carlo method on the basis of IEC60627 [11–13].

In the present study, we used three factors—modulation transfer function (MTF), normalised noise power spectrum (NNPS) and detective quantum efficiency (DQE) to quantitatively assess the effect of different grid ratios on image quality. Furthermore, we proposed a standard for selecting an optimised grid ratio for each DR system on the basis of our results.

Methods and materials

Experiment method

X-ray tubes (Model: E7252X, Toshiba, Japan) with a tube voltage range of 40–150 kV, maximum current of 400 mA and 1000 mA and focal spot of 0.6 mm and 1.2 mm were used in this study. A flat panel detector (Model: FDX3543RP, Toshiba, Japan) (with Csl scintillator) with pixel size of 143 μm and pixel matrix of 2448 × 2984 was used. SID was set at 100 cm, which is a commonly used setting, to evaluate effect of grid ratio in the clinical setting [14]. Aluminum interspaced grids by JPI Healthcare (Seoul, Republic of Korea) were used. To minimise image distortion caused by the grid, an optimised grid with a line frequency of 85 LP/cm was used and the FD was set to 100 cm, which was identical to the SID value, to prevent cutoff caused by the use of unmatched FD. Experiments were conducted under four different grid ratio conditions: 1) without grid, 2) 10:1, 3) 12:1 and 4) 15:1. For each ratio, images were acquired and analysed for changes in image quality depending on the grid ratio.

Two phantoms were used in the experiments (Fig. 3): poly methyl methacrylate (PMMA), edge phantom. The PMMA phantom with dimensions of 25 cm × 25 cm × 1 cm was primarily used to artificially adjust the amount of scattered radiation that reaches the detector by changing the number of layers. The edge phantom, made of tungsten, was used to measure MTF.

The experimental setup is shown in Fig. 4. The X-ray tube was placed vertically to and in the center of a flat panel detector. A jig was created and used to avoid the effect of movement of phantoms or grids on results. The radiation exposure was measured by placing a dosimeter at the center of the detector. RQA 5 condition (70 kVp, 21 mm Aluminum filter) of IEC 61267, recommended by IEC 62220-1 for the X-ray condition, was used. Table 1 shows mAs of X-rays used per unit thickness of the PMMA phantom used in the experiment and

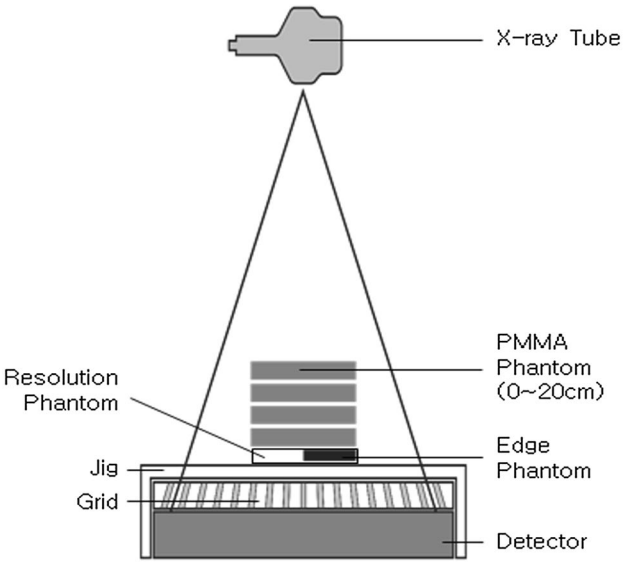

Fig. 4 Experimental setup

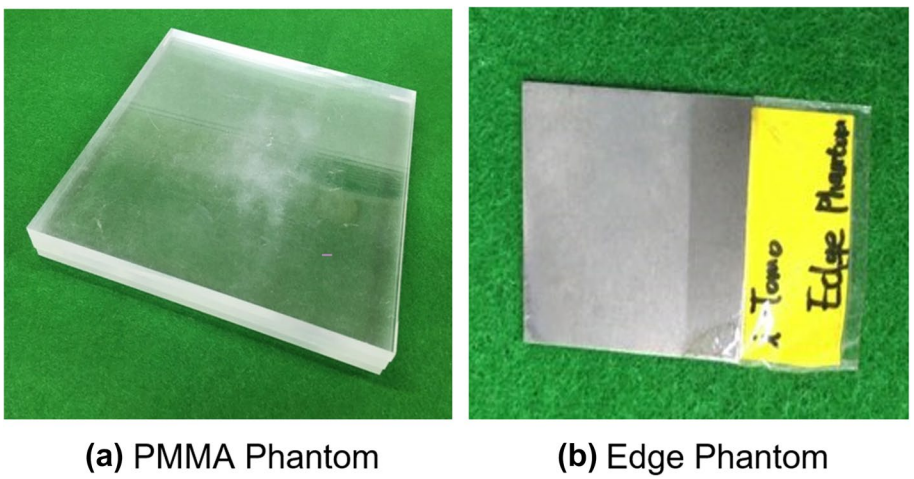

Fig. 3 Phantoms used in the experiment

Table 1 X-ray exposure conditions and grid specification

No	PMMA thickness (cm)	Grid line density (LP/cm)	Grid ratio	Bucky factor (@ RQR 8)	MAs
1	0	85	Without grid	–	2
2			10:1	2.33	2.8
3			12:1	2.60	
4			15:1	2.96	
5	10	85	Without grid	–	11.2
6			10:1	2.33	25
7			12:1	2.60	
8			15:1	2.96	
9	20	85	Without grid	–	56
10			10:1	2.33	160
11			12:1	2.60	
12			15:1	2.96	

Bucky factor of used grid. To prevent any unexpected effect of image processing, only raw images were used in the analysis.

Analysis method

We quantitatively analysed changes in image quality with varying grid ratios using MTF, NNPS and DQE analyses. MTF, NNPS and DQE were measured based on the IEC62220-1 standard [15].

MTF is a criterion for evaluating the resolution and sharpness of an X-ray system: the higher the MTF, the higher the resolution and sharpness. Figure 5 shows the MTF analysis process using the edge phantom image.

To compute MTF, a region of interest (ROI) is first extracted around the edge of the edge phantom image, followed by acquiring the edge spread function (ESF) using the profile penetrating the edge of ROI. Next, line spread function (LSF) is obtained by differentiating the acquired ESF. Finally, the MTF curve is acquired by applying Fourier transform function to LSF [15–18]. In Fig. 5a, the direction of the line profile is parallel to the direction of the grid line.

The DQE reflects how effectively a DR system can generate a signal-to-noise ratio (SNR) of image according to frequency relative with ideal detector. Thus, increase in DQE reduces the dose necessary to acquire an image of the same SNR. As a result, the dose to be irradiated to the patient can be reduced. DQE can be calculated using the equation below [15, 19–21].

$$DQE(f) = \frac{SNR_{out}^2}{SNR_{in}^2} = \frac{MTF(f)^2}{q \times X \times NNPS(f)} \quad (1)$$

where, SNR_{in} signal-to-noise ratio of the detector input signal, SNR_{out} signal-to-noise ratio of the detector output signal, radiation exposure(Unit: μGy), NNPS(f) normalised noise power spectrum by frequency, q incidental number of X-ray photon per unit area (RQA 5: 30 174 quanta/μGy mm^2).

Here, the MTF value was calculated using the method mentioned earlier.

The NPS is one of the most common factor describing the noise properties of DR system. NPS is a representation of the distribution of the noise variance on the spatial frequencies, indicating the dependence on the spatial frequency of noise, which is a variation between pixels in the image [20, 22–24]. NNPS was calculated by the following equation:

$$NPS(f) = \frac{< |FT(I(x,y)) - S(x,y)|^2 >}{N_x \times N_y} \times p_x \times p_y \quad (2)$$

$$NNPS(f) = \frac{NPS(f)}{(\text{Large area signal})^2} \quad (3)$$

where, I(x, y) X-ray image, S(x, y) average image of X-ray images, N_x, N_y number of pixels of the x-axis and y-axis, p_x, p_y pixel size of the x-axis and y-axis, NPS(f) noise power spectrum by frequency, Large area signal: mean value of the pixels used in the calculation of NPS.

Results

MTF

Figure 6 and Table 2 show changes in MTF with changed in grid ratio and the thickness of the PMMA phantom. Figure 7a shows MTF without the PMMA phantom. When there is no object to generate scattered radiation, MTF values showed similar characteristic regardless of grid ratio. Figure 7b and c shows the MTF values obtained using the PMMA phantom with thicknesses of 10 cm and 20 cm, respectively. The MTF value increased with the use of a grid is compared with that obtained without the use of a grid, and it increased with increase in grid ratio. When the thickness of the PMMA phantom was 10 cm, the MTF value of the grid with a grid ratio of 10:1 improved by 75.6% compared with the MTF value obtained without the use of a grid (value difference of 17% at 1 LP/mm). The MTF value of the grid with a grid ratio of 15:1 improved by 20.5% compared with the MTF value of the grid with a grid ratio of 10:1 (value difference of 8% at 1 LP/mm). When the thickness of the PMMA phantom was 20 cm, the MTF value of the grid with a grid ratio of 10:1 improved by 141.5% compared with the MTF value obtained without the use of a grid (value difference of 15% at 1 LP/mm). The MTF value of the grid with a grid ratio of 15:1 improved by 33.2% compared with the

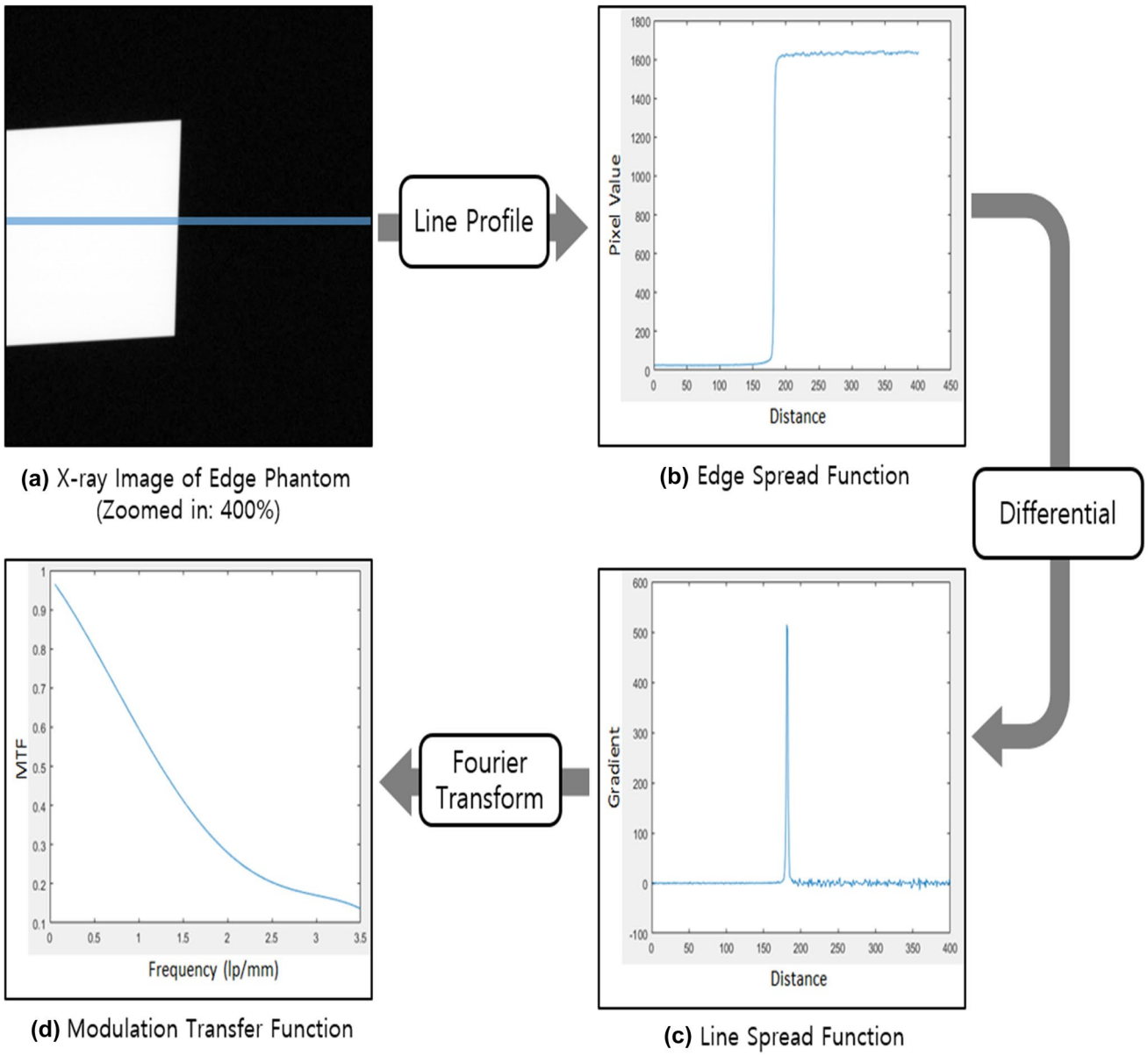

Fig. 5 MTF analysis process using the edge phantom image

MTF value of the grid with a grid ratio of 10:1 (value difference of 8.5% at 1 LP/mm).

NNPS

Figure 7 and Table 2 show changes in NNPS with changes in grid ratio and the thickness of PMMA phantom. Figure 7a–c show the NNPS values obtained using the PMMA phantom with thicknesses of 0, 10 and 20 cm, respectively. The NNPS value increases with the use of a grid compared with that obtained without the use of a grid, and it increased with an increase in grid ratio.

When the thickness of the PMMA phantom was 0 cm, the NNPS value of the grid with a grid ratio of 10:1 improved by 2.7% compared with that obtained without the use of a grid (value difference of 2.23×10^{-7} at 1 LP/mm). The NNPS value of the grid with a grid ratio of 15:1 improved by 13.5% compared with that with a grid ratio of 10:1 (value difference of 1.15×10^{-6} at 1 LP/mm). When the thickness of the PMMA phantom was 10 cm, the NNPS value of the grid with a grid ratio of 10:1 improved by 24.1% compared with that obtained without the use of a grid (value difference of 1.47×10^{-6} at 1 LP/mm). The NNPS value of the grid with a grid ratio of 15:1 improved by 34.0% compared with that with a grid ratio of 10:1

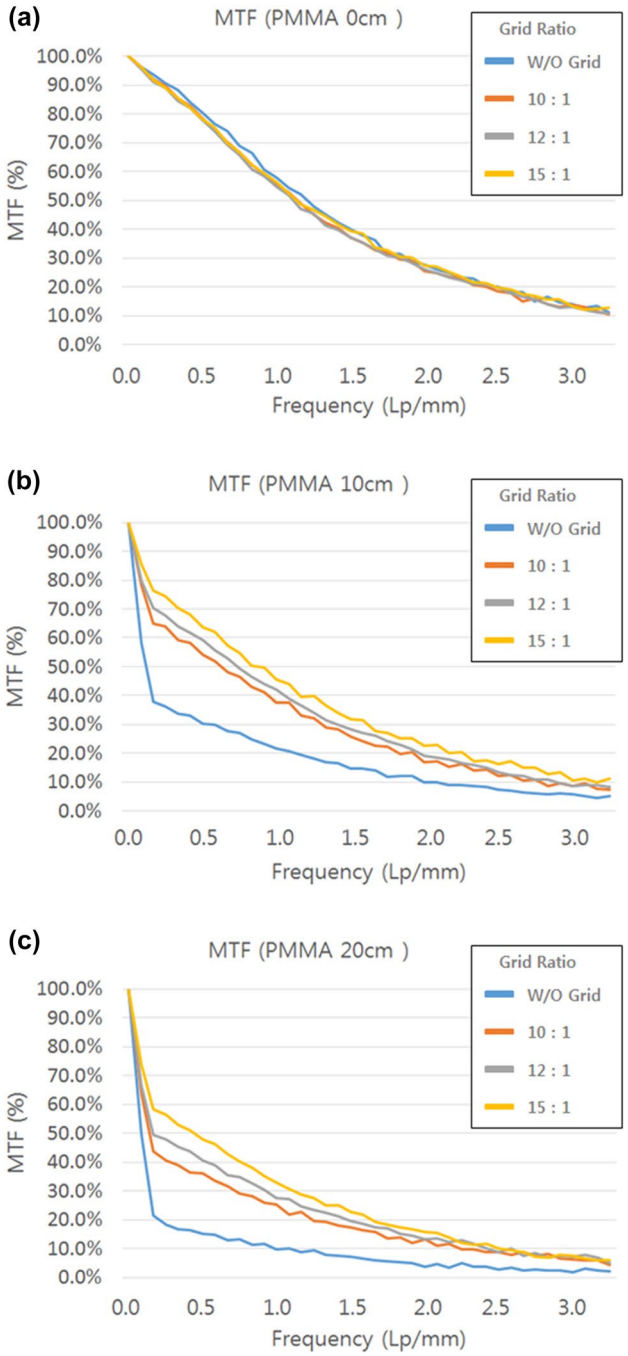

Fig. 6 Change in MTF characteristics with changes in PMMA thickness and grid ratio

(value difference of 2.56×10^{-6} at 1 LP/mm). When the thickness of the PMMA phantom was 20 cm, the NNPS value of the grid with a grid ratio of 10:1 improved by 59.4% compared with that obtained without the use of a grid (value difference of 3.67×10^{-6} at 1 LP/mm). The NNPS value of the grid with a grid ratio of 15:1 improved by 59.7% compared with that with a grid ratio of 10:1 (value difference of 5.87×10^{-6} at 1 LP/mm).

DQE

Figure 8 and Table 2 shows changes in DQE with changes in grid ratio and the thickness of PMMA phantom. Figure 8a is the graph of DQE without using the PMMA phantom. When there is no object to generate scattered radiation, the DQE values showed similar characteristics regardless of grid used. The DQE value was not affected by grid in the case of no subject to generate scattered radiation. Figure 8b and c shows DQE values obtained using the PMMA phantom with thicknesses of 10 cm and 20 cm, respectively. The DQE value increases with the use of a grid compared with that obtained without the use of a grid, and it increased with increase in grid ratio.

When the thickness of the PMMA phantom was 10 cm, the DQE value of the grid with a grid ratio of 10:1 improved by 256.6% compared with the DQE value obtained without the use of the grid (value difference of 13.6% at 1 LP/mm). The DQE value of the grid with a grid ratio of 15:1 improved by 59.3% compared with the DQE value of the grid with a grid ratio of 10:1 (value difference of 11.2% at 1 LP/mm). When the thickness of the PMMA phantom was 20 cm, the DQE value of the grid with the grid ratio of 10:1 improved by 600% compared with the DQE value obtained without the use of the grid (value difference of 5.4% at 1 LP/mm). The DQE value of the grid with a grid ratio of 15:1 improved by 76.2% compared with the DQE value of the grid with a grid ratio of 10:1 (value difference of 4.8% at 1 LP/mm).

Discussion

In this study, we investigated effects of grid ratio on the quality of images obtained using a DR system in the clinical setting. The line frequency of the grid was set at 85 LP/cm, which is an optimised setting for the detector used in this research. Images were obtained under four different grid ratio conditions: without a grid and with grids at 10:1, 12:1, or 15:1. To obtain images under various conditions of scattering, we changed the thickness of the PMMA phantom from 0 to 20 cm. Images were quantitatively evaluated by MTF, DQE and NNPS using several evaluation criteria.

Changes in MTF and DQE values depending on the thickness of the PMMA phantom and grid ratio showed similar trends. When the PMMA phantom was not used, MTF and DQE showed a decreasing trend depending on spatial resolution regardless of the use of a grid. In contrast, MTF and DQE rapidly decreased with increase in the thickness of the PMMA phantom. However, MTF and DQE all improved when a grid was used, and a higher grid ratio resulted in a greater improvement. On the other hand, the NNPS increased when using the grid, regardless

Table 2 MTF, NNPS and DQE by frequency according to PMMA thickness and grid ratio

Ratio	MTF (at 1 LP/mm)			NNPS (at 1 LP/mm)			DQE (at 1 LP/mm)		
	PMMA 0 cm (%)	PMMA 10 cm (%)	PMMA 20 cm	PMMA 0 cm (mm^2)	PMMA 10 cm (mm^2)	PMMA 20 cm (mm^2)	PMMA 0 cm (%)	PMMA 10 cm (%)	PMMA 20 cm (%)
Without grid	59.4	22.5	10.6	8.30×10^{-6}	6.07×10^{-6}	6.18×10^{-6}	43.7	5.3	0.9
10:1	57.2	39.5	25.6	8.52×10^{-6}	7.54×10^{-6}	9.84×10^{-6}	41.3	18.9	6.3
12:1	56.6	43.0	28.9	9.09×10^{-6}	8.62×10^{-6}	1.20×10^{-5}	40.4	23.1	8.2
15:1	57.9	47.6	34.1	9.67×10^{-6}	1.01×10^{-5}	1.57×10^{-5}	43.0	30.1	11.1

of the PMMA phantom use. And the higher the ratio of grid, the more NNPS increased.

MTF is one of the most important factors for evaluating the sharpness and resolution of images obtained using a DR system. Increase in the MTF value indicates increase in the sharpness of the image. Because MTF decreased as the thickness of the PMMA phantom increases, we can assume that scattered X-rays have a significant effect on the resolution and sharpness of images obtained using a DR system and that increase in the amount of scattered X-rays leads to rapid deterioration of the resolution and sharpness of an image. Moreover, the use of high-ratio grids may contribute to the resolution and sharpness images obtained using a DR system because more scattered X-rays are removed with higher grid ratio.

NNPS is an important factor in describing the noise characteristics of the DR system. When grid use in the DR system, the NNPS of the image was increased due to the reduction of the incident dose to the detector. In addition, the NNPS increased as the grid ratio increased.

DQE is an important factor indicating how effectively a DR system can generate a SNR relative to an ideal detector. Scattered X-rays are increased as the thickness of the PMMA phantom increases, negatively affecting DQE. The use of a grid improves the high-SNR image generation efficiency of the DR system, and this improvement was greater when a high-ratio grid was used.

As a result, the DR system using a grid for acquiring patients' images may increase the noise slightly, but it improves the image quality and enables high-SNR image acquisition. Furthermore, higher grid ratios lead to greater improvement in image quality. Therefore, we assume that it is desirable to use a high-ratio grid for better DR image quality in the clinical setting. Of note, a study is being conducted on the use of a smaller amount of emitted X-rays to reduce patient dose while obtaining images using a DR system in a clinical setting. In future studies, we will address changes in image quality and dose depending on grid ratio.

Conclusion

This study quantitatively assessed changes in the quality of images obtained using a DR system depending on grid ratio using three image quality evaluation methods (MTF, NNPS and DQE). To quantitatively analyse the effect of grid ratio on the removal of scattered X-rays in a clinical setting, we used a PMMA phantom (thicknesses ranging from 0 to 20 cm) to simulate various conditions of scattered X-rays. Referring to MTF and DQE by frequency according to PMMA thickness and grid ratio of Table 2, when there were no scattered X-rays (PMMA thickness 0 cm), MTF and DQE showed similar trends regardless of the use of a grid. However, when scattered X-rays were generated using the PMMA phantom with a thickness of 10 or 20 cm, MTF and DQE acquired with the use of a grid had better MTF and DQE than those acquired without the use of a grid. The NNPS increased regardless of PMMA thickness when using the grid. At 20 cm PMMA thickness, a ratio grid of 15:1 improved MTF by 222%, NNPS by 154% and DQE by 1133% compared with images acquired without the use of a grid. The increase in MTF and DQE was higher than the increase in NNPS. Therefore, it is necessary to use a grid for accurate diagnosis in a clinical environment, and it is highly recommended to use a high-ratio grid.

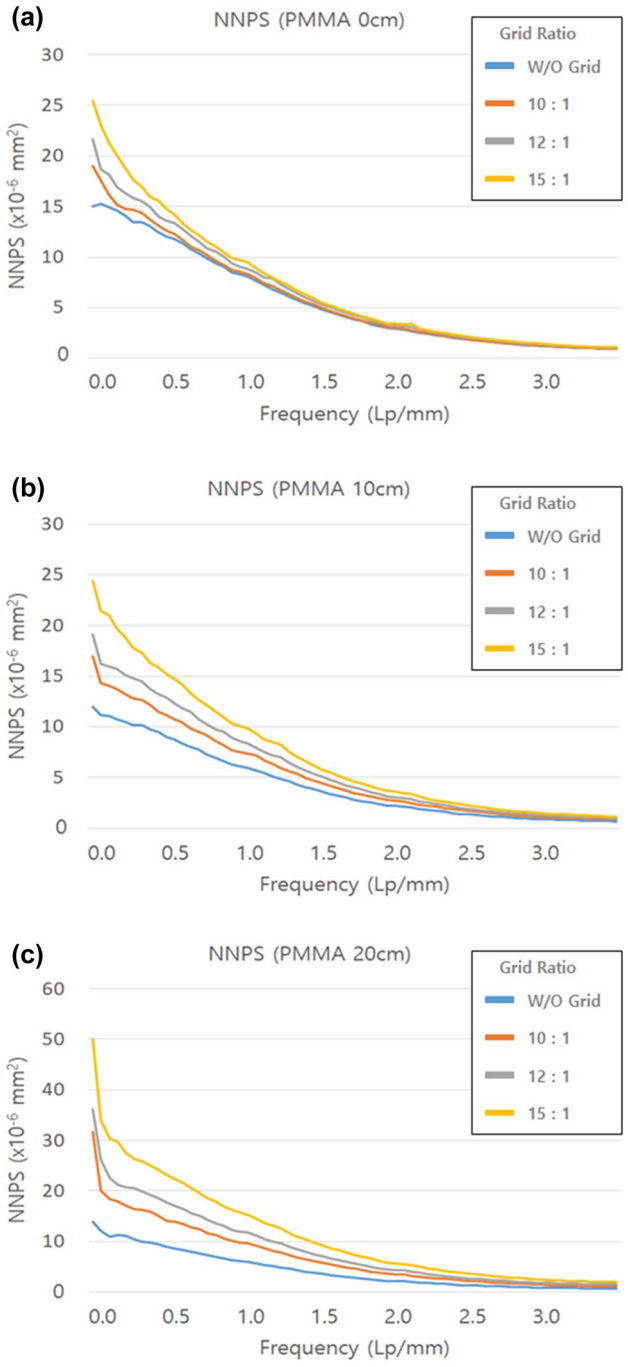

Fig. 7 Change in NNPS characteristics with changes in PMMA thickness and grid ratio

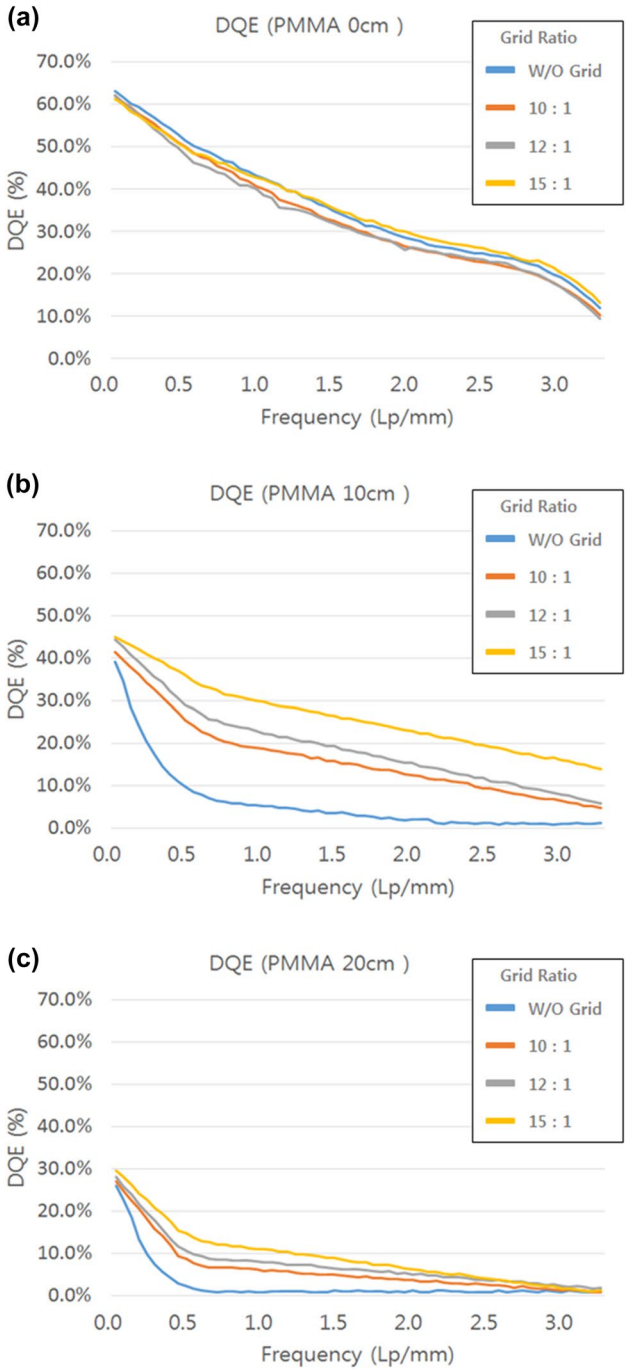

Fig. 8 Change in DQE characteristics with changes in PMMA thickness and grid ratio

Compliance with ethical standards

Conflict of interest The authors of this manuscript declare relationships with JPI Healthcare, Co., Ltd., and the authors state that this work has not received any funding.

Research involving human participants and/or animals We did not perform direct experiments on humans or animals. Results of prior human radiological studies were selected.

Informed consent Informed consent was obtained from all participants in the study.

References

1. Bucky G (1913) A grating-diaphragm to cut off secondary rays from the object. Arch Roentgen Ray 18:6–9. https://doi.org/10.1259/arr.1913.0005
2. Hondius Boldingh W (1964) Grids to reduce scattered X-rays in medical radiography. Technische Hogeschool Eindhoven, Eindhoven. https://doi.org/10.6100/IR62689
3. Tang C-M, Stier E, Fischer K, Guckel H (1998) Anti-scattering X-ray grid. Microsyst Technol 4:187–192. https://doi.org/10.1007/s005420050128
4. Hendee William R, Russell Ritenour E (2002) Medical imaging physics. Radiography, 4th edn. Wiley, New York, pp 217–234
5. Belykh I (2014) Grid artifacts suppression in computed radiographic images. Int J Biomed Biol Eng 8:1402–1405
6. Papp Jeffrey (2014) Quality management in the imaging sciences, 5th edn. Elsevier, Maryland
7. Yoon Jai-Woong, Park Young-Guk, Park Chun-Joo, Kim Do-Il, Lee Jin-Ho, Chung Nag-Kun, Choe Bo-Young, Suh Tae-Suk, Lee Hyoung-Koo (2007) Reduction of a grid moiré pattern by integrating a carbon-interspaced high precision X-ray grid with a digital radiographic detector. Med Phys 34:4092–4097. https://doi.org/10.1118/1.2775743
8. Belykh I, Cornelius CW (2001) Antiscatter stationary-grid artifacts automated detection and removal in projection radiography images. In: Proceedings of the SPIE 4322, Medical imaging 2001: Image processing, pp 1162–1166 https://doi.org/10.1117/12.430992
9. International Electrotechnical Commission (2013) IEC 60627:2013, Diagnostic X-ray imaging equipment: characteristics of general purpose and mammographic anti-scatter grids, 3rd edn. International Electrotechnical Commission, Geneva
10. JPI Healthcare (2015) JPI's grid book, 7th edn. JPI Healthcare, Ansan-si
11. Khodajou-Chokami H, Sohrabpour M (2015) Design of linear anti-scatter grid geometry with optimum performance for screen-film and digital mammography systems. Phys Med Biol 60:5753–5766. https://doi.org/10.1088/0031-9155/60/15/5753
12. Ghaffarian P, Sharafi AA, Keshavarz K, Zaidi H (2005) MCNP4C-based Monte Carlo study of grid performance in diagnostic radiology. Biomed Tech 50:1098–1099
13. Woo-HyunChung Sang-HyunLee (2018) Study of Monte Carlo simulator for estimation of anti-scatter grid physical characteristics on IEC 60627:2013-based. Am J Phys Appl 6:35–42. https://doi.org/10.11648/j.ajpa.20180602.12
14. Kenneth L, Bontrager MA, Lampignano J (2013) Textbook of radiographic positioning and related anatomy, 8th edn. Elsevier, Maryland
15. International Electrotechnical Commission (2003) IEC62220-1:2003, Medical electrical equipment – Characteristics of digital X-ray imaging devices – Part 1: determination of the detective quantum efficiency, 1st edn. International Electrotechnical Commission, Geneva
16. Neitzel Ulrich, Buhr Egbert, Hilgers Gerhard, Granfors Paul R (2004) Determination of the modulation transfer function using the edge method: influence of scattered radiation. Med Phys 31:3485–3491. https://doi.org/10.1118/1.1813872
17. Samei Ehsan, Flynn Michael J (2003) An experimental comparison of detector performance for direct and indirect digital radiography systems. Med Phys 30:608–622. https://doi.org/10.1118/1.1561285
18. Samei Ehsan, Flynn Michael J, Reimann David A (1998) A method for measuring the presampled MTF of digital radiographic systems using an edge test device. Med Phys 25:102–113. https://doi.org/10.1118/1.598165
19. Gupta Arun Kumar, Chowdhury Veena, Khandelwal Niranjan (2013) Diagnostic radiology: recent advances and applied physics in imaging, 2nd edn. Jaypee Brothers Medical Pub, New Delhi
20. Van Metter Richard L, Beutel Jacob, Kundel Harold L (2000) Handbook of medical imaging volume 1 physics and psychophysics. Applied linear-systems theory. SPIE Press, Bellingham, pp 79–160
21. Ranger NT, Samei E, Dobbins JT 3rd, Ravin CE (2007) Assessment of detective quantum efficiency: intercomparison of a recently introduced international standard with prior methods. Radiology 243:785–795. https://doi.org/10.1148/radiol.2433060485
22. Zhou Zhongxing, Gao Feng, Zhao Huijuan, Zhang Lixin (2011) Techniques to improve the accuracy of noise power spectrum measurements in digital X-ray imaging based on background trends removal. Med Phys 38:1600–1610. https://doi.org/10.1118/1.3556566
23. Williams Mark B, Mangiafico Peter A, Simoni Piero U (1999) Noise power spectra of images from digital mammography detectors. Med Phys 26:1279–1293. https://doi.org/10.1118/1.598623
24. Dong Sik Kim (2016) Noise power spectrum measurements in digital imaging with gain nonuniformity correction. IEEE 25:3712–3722. https://doi.org/10.1109/TIP.2016.2574985